High-resolution electro-chemical transistors defined by mould-guided drying of PEDOT:PSS liquid suspension

Jin Li, [†] *Xin Chang,* [†] *Shunpu Li,* [†,‡] *Pawan Kumar Shrestha,* [†] *Edward K.W. Tan,* [§] *and Daping Chu*,*[†]

† Centre for Photonic Devices and Sensors, University of Cambridge, 9 JJ Thomson Avenue, Cambridge CB3 0FA, UK

‡ College of New Materials and New Energies, Shenzhen Technology University, Shenzhen, 518118, China.

§ Department of Engineering, University of Cambridge, Cambridge, CB3 0FA, UK

KEYWORDS: PEDOT:PSS liquid suspension; mould-guided drying; electro-chemical transistors; short channels; small-scale devices

ABSTRACT: Ion-sensitive transistors with nano- or micro- scale dimensions are promising for high-resolution electrophysiological recording and sensing. Technology that can pattern polymer functional materials directly from solution can effectively avoid any chemical damage induced by conventional lithography techniques. The application of mould-guided drying technique to

pattern PEDOT:PSS-based transistors with high resolution directly from the water-based suspension is presented in this paper. Gold electrodes with short channels were firstly defined by creating high-resolution polymer lines with mould-guided drying, followed by pattern transfer through a lift-off process. Then PEDOT:PSS lines were subsequently created through identical mould-guided drying process on the predefined electrodes. Small-scale transistor devices with both shortened channel length and width exhibited a good high-frequency response because of the weak capacitive effect. This is particularly advantageous for electrochemical transistors since the use of conventional fabrication techniques is extremely challenging in this case. In addition, modified polymer chain alignment of the assembled PEDOT:PSS lines during the drying process was observed by optical and electrical measurement. The mould-guided drying technique has been proved to be a promising method to fabricate small-scale devices, especially for biological applications.

1. Introduction

Recent developments in solution-processable devices/systems have revived interest in micrometer- and nanometer- scale drying process. Considerable efforts have been made to generate high-resolution patterns or structures using various methods including (a) controlling solvent evaporation, such as inkjet printing [1,2], (b) line-wise deposition by pulling a sharp blade [3-5], and (c) repeated pinning / depinning of the contact line between the drying solution and substrate [6-8]. Edge deposition induced by template confinement has also been used to form high-resolution structures including the progressive shrinkage of capillary bridge and groove pinning [9-11]. Direct patterning of materials from solution has several advantages: high resolution, inexpensive cost, and applicability to a range of situations where conventional lithography

technology may not be suitable due to the induced material degradation by UV irradiation and chemical reaction during the development process.

Fine patterning of ion-sensitive materials to form small-sized devices that permit high-frequency detection and high-density device packing is undoubtedly attractive. For instance, a small ion-sensitive transistor array can be used for high-resolution bio-recording where the ion concentration fluctuates within the subcellular domain [12, 13]. Ion-based synaptic transistors with a proper dopant in the active layer could generate reprogrammable and multiple states with stable conduction which are promising for next-generation neuromorphic computing, and the miniaturization of such synaptic transistors is significant for large-scale integration [14].

Poly (3,4-ethylenedioxythiophene)-poly (styrenesulfonate) (PEDOT:PSS) is a well-known conducting polymer which is a blend of cationic polythiopene derivatives doped with a polyanion [15-17]. The polymer conductance is extremely sensitive to ions doping from the environment by modifying the redox conditions of the PEDOT polymer [18-20]. Various techniques have been used to patterning PEDOT:PSS materials which includes mask etching [11, 21, 22], soft-lithography [23], nanoimprint [24], pulsed laser ablation [25], direct UV-patterning [26], selective polymerization [27,28] and electro-spin [29]. Most of the approaches are mainly limited by insufficient spatial resolution. Although electro-spin, nanoimprint and mask etching techniques can be used to produce sub-micron PEDOT:PSS, they demand further pattern transfer by plasma etching or face challenges to form a well-defined pattern. To this end, the development of techniques that enable direct patterning of PEDOT:PSS with high resolution is valuable.

In this paper, a novel patterning process based on the mould-guided drying technique [11] was used in this paper to pattern PEDOT:PSS directly from its water suspension and to fabricate

PEDOT:PSS-based organic electrochemical transistors (OECTs). In the process, gold electrodes with narrow channels were firstly defined by creating polymer lines with mould-guided drying technique and transferring the pattern through a lift-off process. Then, the mould-guided drying process was repeated to form PEDOT:PSS lines over the electrodes through proper solution formulation. The OECT with both shortened channel length and width, demonstrated good high-frequency and multi-frequency responses. In addition, the alignment of PEDOT:PSS chains during formation of the assembled lines was observed and it was confirmed by electrical and optical measurements.

2. Results and Discussion

2.1. Principle of PEDOT:PSS patterning

The formation process used for PEDOT:PSS patterning is schematically shown in Figure 1. A formulated PEDOT:PSS water suspension was introduced between a substrate and a polydimethylsiloxane (PDMS) mould. As the solvent evaporated, capillary bridges of the solution formed and the liquid / substrate contact lines were pinned at the mould grooves. Thin PEDOT:PSS lines were subsequently formed next to the groove-pinned contact lines. To be more specific, a controlled volume of the formulated solution (~3μl, for PDMS mould with 1cm^2 area of line pattern) was drop-casted onto the surface of the structured PDMS mould. Then, a substrate was gently brought into contact with the solution-wetted mould and left dried at room temperature for 4 hours under a small applied pressure (about 5 MPa) (Figure 1a and Figure 1b). Finally, the PDMS mould was removed, leaving the patterned PEDOT:PSS on the substrate (Figure 1c). The groove depth of the PDMS mould was 1.5μm and the line width / separations varied from 40μm to 120μm.
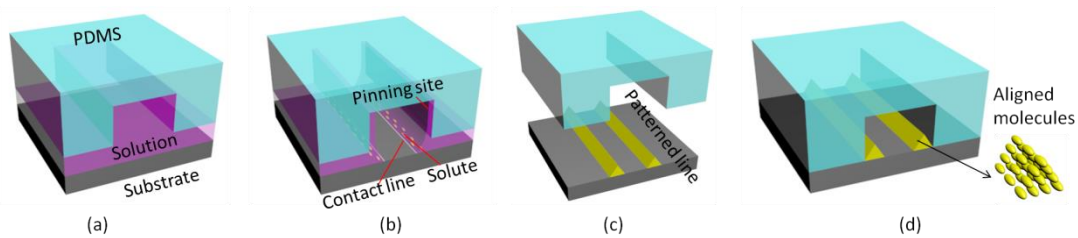
Figure 1 Schematic illustration of PEDOT:PSS patterning process. The solution was patterned and subsequently pinned at the groove corners during drying (a, b). The PEDOT:PSS lines were formed next to the liquid / substrate contact lines (b, c). The PEDOT:PSS line deposition induced by capillary flow causes a preferred PEDOT chain orientation (d).

The PEDOT:PSS lines were formed by a single patterning process (Figure 2a) and a sequential double patterning process can be used to generate grid structures (Figure 2b). The existing structure on the substrate does not affect the subsequent patterning because the capillary bridges are pinned at the mould grooves. We also observed that the PEDOT:PSS solution formulation was critical for the successful patterning, which was discussed in section 4. Apart from the modification of the surface property of the substrate and surface tension of the solution, both ethylene glycol and triton can affect polymer chain alignment and interaction between the PEDOT and PSS molecules which might contribute to the patterning process and the resulted structures [30]. The typical line width was measured to be 700nm and the width of PEDOT:PSS wires can be controlled by adjusting the solution concentration. It was also found that the profile of the patterned PEDOT:PSS wire was approximately triangle.
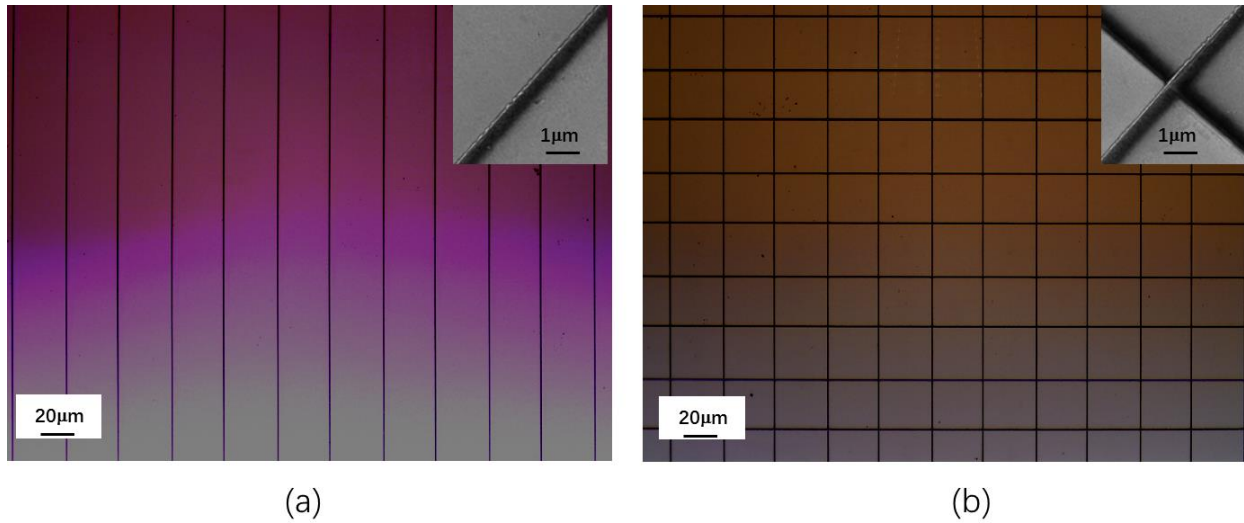
Figure 2. Optical and SEM images of the patterned PEDOT：PSS lines (a) and grids (b). The typical line width was 700nm.

2.2. PEDOT:PSS wire transistors

The PEDOT:PSS-based OECT was fabricated by firstly preparing electrodes with small gaps using a similar process. Silicon with a 300 nm-thick SiO_2 layer or glass was used as the substrate. A 250 nm-thick polydimethylglutarimide (PMGI) layer was spin-coated on the substrate and baked for 30 min at 200°C. A 10 nm-thick Ge layer was then thermally evaporated on top as an etching mask (in CF_4) for subsequent PMGI etching (in oxygen). . Poly-4-vinylphenol (PVP) lines were formed on the Ge layer using the method described in Figure 3a. CF_4 plasma was used to etch through the Ge layer with PVP line as the etching mask and this was followed by oxygen plasma to etch through the PMGI using Ge layer as the etching mask (Figure 3b). Then, Au / Cr (30 nm / 10 nm) films were deposited by thermal evaporation and the lift-off process in a Microposit Remover (1165) was applied to complete the electrode fabrication (Figure 3c) [31,32].

Finally, PEDOT:PSS lines were created on top of the fabricated Au electrodes (Figure 3d) and annealed at 140°C for 1 hour in air.
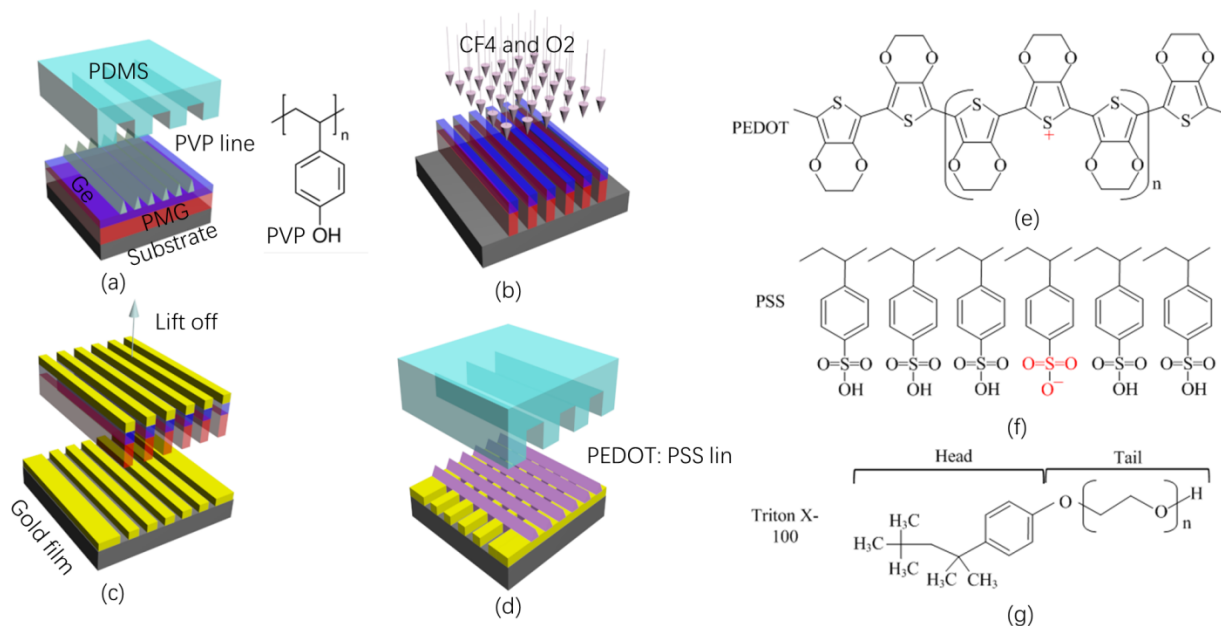

Figure 3. Process used for the fabrication of PEDOT:PSS-based OECT (a~d) and molecular structure of PEDOT:PSS polymers and Triton X-100 (e, f, g)

Figure 4a and 4b show the device image and testing circuit used for device characterization. Silver conducting wire and 0.1 M NaCl aqueous solution were used as the gate electrode and electrolyte respectively. A plastic ring (6 mm in diameter) was placed over the sample to contain the electrolyte. The transistors were evaluated under small gate and drain voltages (<1V). The drain current decreased as the gate voltage increased, i.e., the device worked with a depletion model because of the partial balance of the negatively charged PSS$^-$ by Na+ which de-dopes the PEDOT (Fig 4c, 4d). The OECT with a small size is crucial for high-resolution sensing, like bio-recording, where the ion concentration varies within the subcellular domain. Due to the short

device channel, the current density was one order of magnitude higher than that with the PEDOT:PSS-wires defined by mask etching [11].
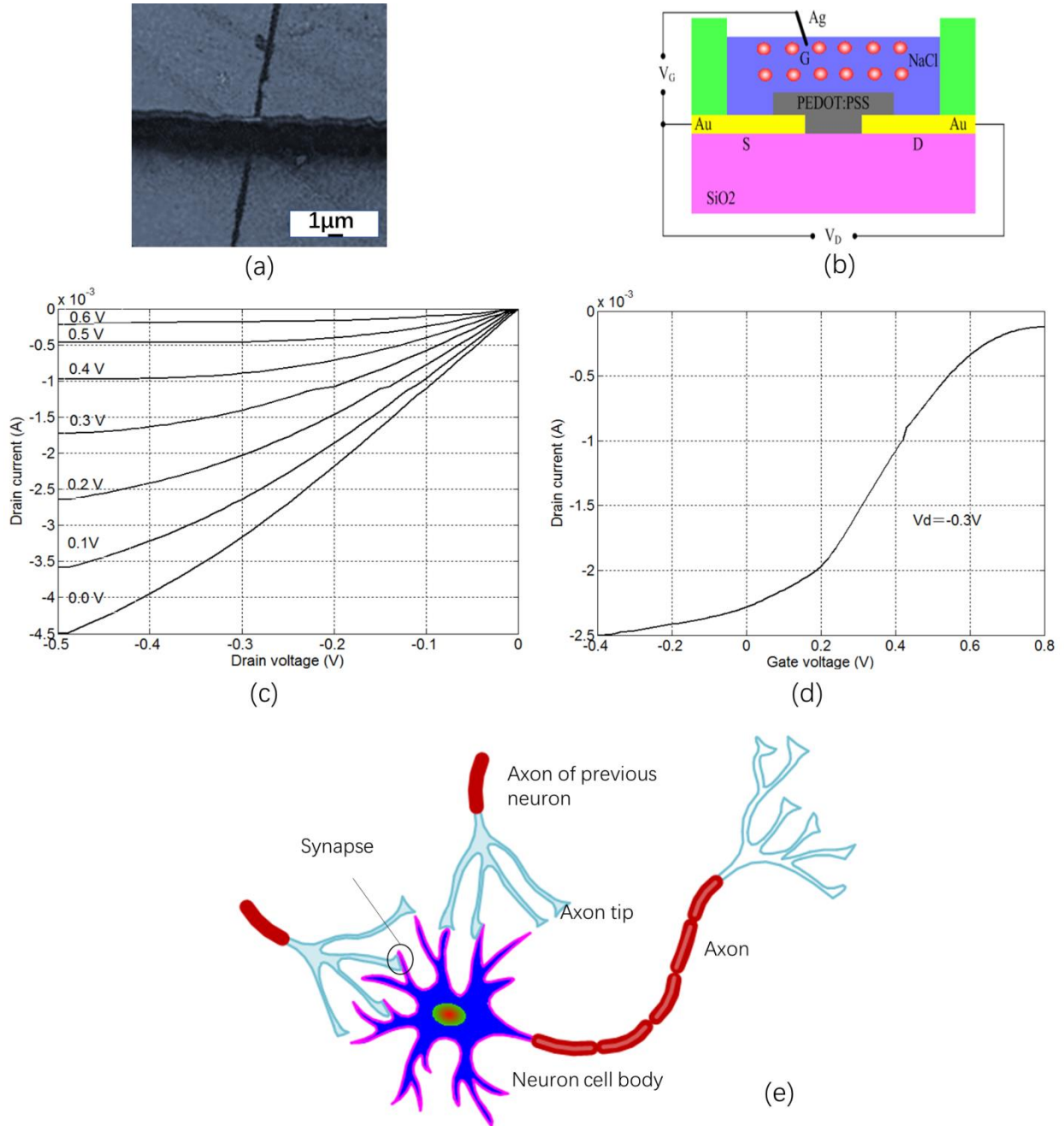

(a)

(b)

(c)

(d)

(e)

Figure 4. Fabricated device image and test results. (a) SEM image of a fabricated device; (b) Schematic illustration of the testing circuit; (c) and (d) Output and transfer curves of the OECT;

(e) Schematic illustration of signal transformation between neurons where two pre-synapse neurons and one post-synapse neuron were drawn. This is analogous to the two-input and one-output structure of OECT device.

PEDOT:PSS-based OECT with small size is also promising in applications like synaptic device which is an essential component in artificial neuromorphic network (ANN). Figure 4e shows the schematic illustration of signal transformation between neurons through synapses. The OECT can realize a similar function when the gate voltage and the drain current are analogically treated as pre-synaptic and post-synaptic signals [14].

2.3. Frequency response of the PEDOT:PSS wire transistor

PEDOT:PSS wire transistor with a narrow channel length and channel width has been successfully fabricated and its switching properties have been demonstrated.   The contact area between the PEDOT:PSS wire and the electrolyte is considerably reduced compared to the spin-coated PEDOT:PSS (Figure 5). As a result, the PEDOT:PSS wire transistor has a smaller capacitance between the electrolyte and the active material. This is particularly important for high-frequency operation since the RC time constant ($\tau=R\times C$) is significantly reduced. In order to investigate the high-frequency response of the PEDOT:PSS wire transistor, experiments were conducted with various gate frequencies. The frequency response was measured with an oscilloscope on the voltage drop across a resistor connected in series in the drain current loop. Figure 6 shows the frequency response of different input signals and the device exhibited a good frequency response. Multiple-input response was also measured, which widely exists in the signal processing in the neuron system (Fig.4e) and can be potentially applied for logical calculation [33, 34]. Multiple inputs were realized by using multiple gates and each gate was

powered by a signal generator. Figure 6a shows the single-input response at 1 KHz, while

Figures 6b~e show the multiple-input responses of the transistor and the simulated results. The

resulting output spectra are well described by a summation of multiple input signals and can be

conveniently decomposed at high accuracy, which makes the response to very small variations

between inputs possible. For instance, a tiny phase change (less than 0.01π) of the inputs can be

read out in the output spectra (Figure 6e). The over 1KHz bandwidth of our OECT is sufficient to

record bio-signal in medical application, like brain mapping [19]. Device performance can be

further improved in future research by adding an insulating layer between the liquid and

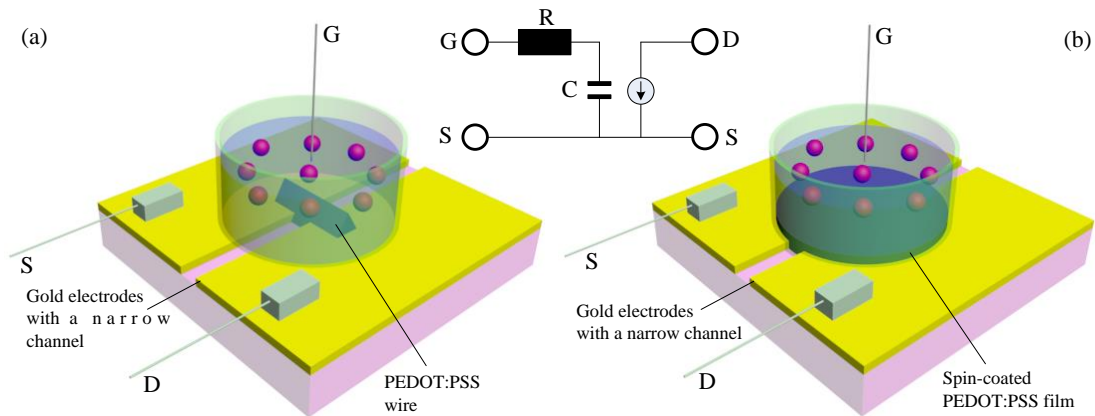electrodes, which is expected to reduce the parasitic effects.

Figure 5. Schematic drawing of transistors with PEDOT:PSS wire (a) and coated PEDOT:PSS
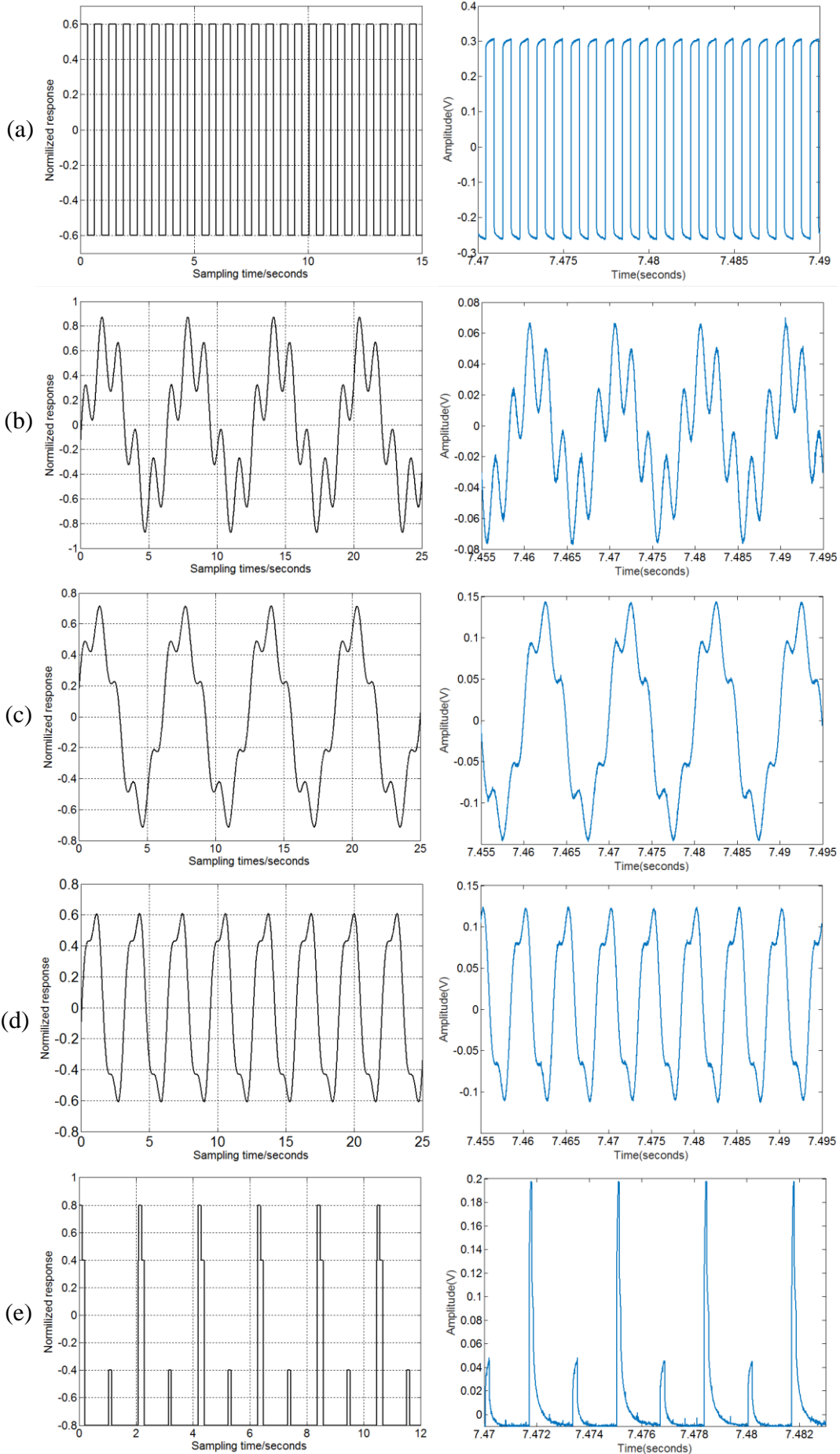
film (b).

Figure 6. Frequency response with sine, square, and pulse signal input, where the left and right panels are the simulated and experimental results respectively. (a) Single square signal (f=1kHz) was the input (the simulated signal is equivalent to the input signal in this case); (b) Two sine signals (f_1=500Hz (600mv), f_2=100Hz (300mv)) were used as the input; (c) Two sine signals (f_1=500Hz (600mv), f_2=100Hz (200mv)) were used as the input; (d) Two sine signals (f_1=500Hz (600mv) and f_2=100Hz (100mv)) were used as the input; (e) Two pulse signals (f_1=500Hz (600mv) and f_2=100Hz (300mv)) with a duty cycle of 10% were used as the input.

2.4. Molecular alignment of PEDOT:PSS wires during formation

The device fabrication and characterization have been presented in the previous sections. Moreover, the molecular alignment of PEDOT:PSS during the guided drying process is expected due to the hydrophobic behavior of PDMS. This was confirmed during the experiment[11] by optical and electrical measurements. Polarized ultraviolet-visible absorption spectroscopy was firstly used to indicate the polymer alignment and a maximum absorption is expected when the transition dipole moments align with the polarization direction of light since the transition dipole moment of the conjugated polymers are oriented in the direction along the polymer backbone [35, 36]. Figure 7 shows the absorbance spectrum of the fabricated PEDOT:PSS wires, in which a larger absorbance was observed when the PEDOT:PSS line direction was oriented parallel to the light polarization direction, indicating that the PEDOT chains are preferentially aligned in the line direction.
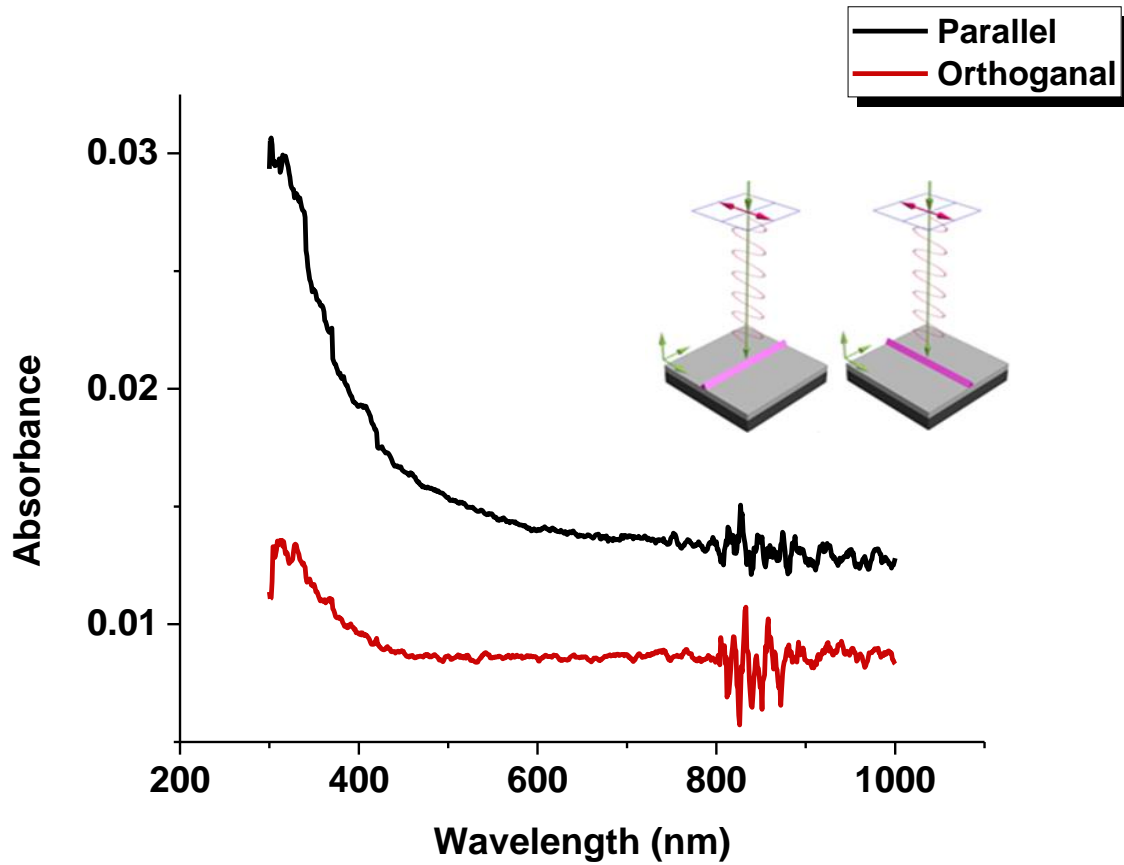
Figure 7 Absorbance of the assembled PEDOT:PSS wires. A larger absorbance is observed when the light polarization direction is parallel to the line orientation.

This was further confirmed by the electrical conductivity of PEDOT:PSS thin film (spin-coating) and PEDOT:PSS wires with identical post treatment (100°C for 10min). The conductivity (σ) of the PEDOT:PSS is calculated by

$$\sigma = \frac{I \times l}{A \times V} \tag{1}$$

where I is the electrical current, l is the conductive length of the PEDOT:PSS, A is the cross-section area and V is the voltage applied. As $I \times l / A = \sigma \times V$, the conductivity ($\sigma$) can be read out

from the slope of $(I \times l/A) \sim V$ plot, as is shown in Figure 8. Moreover, the ratio of conductivity between PEDOT:PSS wires and thin film ($\sigma_{line} / \sigma_{film}$) was extracted to be 2.05, which indicates that the PEDOT:PSS chains were preferentially aligned in the wire direction.
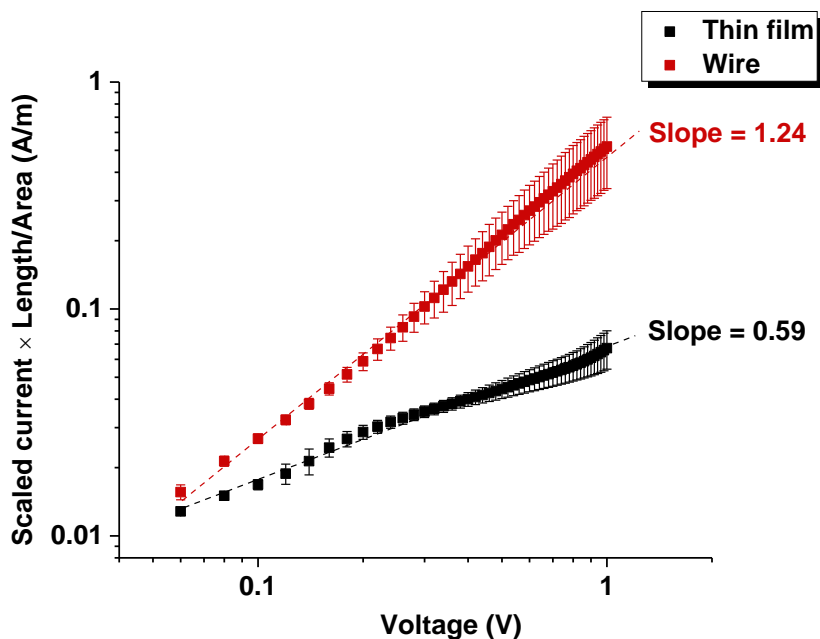

Figure 8 Electrical conductivity of spin-coated PEDOT:PSS thin film and self-assembled

PEDOT:PSS wires.

The preferential alignment of PEDOT chain can be explained by the deposition and collapsing of gel-like particles from the solution [37], as is shown in Figure 9. The PEDOT:PSS dispersion can be regarded as being composed of gel-like particles comprising PSS and PEDOT polymers. The gel-like particles are collapsing and aggregating during the line deposition process. The PEDOT chains are packed either with pure PEDOT chains or PEDOT:PSS chains alternatively in the aggregates [37-39]. The aggregates are connected to form percolation network of charge conduction.

The way of aggregate arrangement and associated global chain-orientation along the PEDOT-lines is required by energy minimization during PEDOT:PSS deposition.
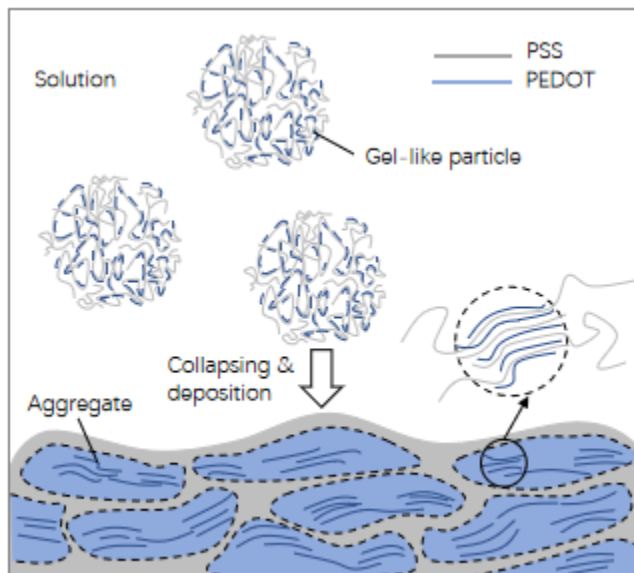

Figure 9 Schematic illustration of PEDOT:PSS deposition from solution. The bottom deposited line is composed by aggregates with PSS rich part (Grey color) and PEDOT rich part (Blue color).

3. Conclusion

We have applied the mould-guided drying process to pattern PEDOT:PSS with high resolution directly from its water-based suspension and small-sized OECT was successfully fabricated. The transistor characteristics of the OECT with small-scale channel width and channel length were demonstrated, and its high-frequency and multiple-input response were also investigated. In addition, PEDOT:PSS chain alignment of the assembled lines was observed and verified by optical and electrical measurement. Such ion-sensitive transistors with small dimensions are particularly promising for high-resolution electrophysiological recording and sensing.

4. Experimental method

Template preparation and line forming: The PDMS template with proper line patterns was made with commercial silicone elastomer (Sylgard ®184, Dow Corning). The silicone elastomer, consisted of a two-part liquid component kit (a 10:1 mix ratio), was poured onto a photoresist master predefined by optical lithography. The thickness of the photoresist carried on Si wafer was 1.5 μm which defines the groove depth of the PDMS template. After curing of the silicone elastomer along with the photoresist master at 70 °C for 1h, the PDMS elastomer with duplicated pattern was peeled-off from the master. PEDOT:PSS and PVP patterning was performed with self-developed stainless-steel clamping platform, which enabled the proper alignment of the substrates and PDMS template, and adjustment of the applied pressure.

Device fabrication and measurements: To fabricate the patterned PEDOT:PSS wire transistors, the PEDOT:PSS solution was formulated with a PEDOT:PSS (Clevios PH-1000) water-based suspension (from Heraeus) by adding 20% ethylene glycol and 0.92% Triton X-100 (Sigma-Aldrich) (both in volume percentage) to PEDOT:PSS suspension in order to improve material conductivity and reduce the surface tension. It was observed that the PEDOT:PSS solution formulation was critical for the PEDOT:PSS patterning, which is the reason why direct patterning of PEDOT:PSS could not be previously achieved by mould-guided drying. The pattern quality is particularly sensitive to the amount of Triton X-100 added to the solution. It was found that a high-quality pattern is obtained when 0.92mg/mL of Triton X-100 was contained in the formulated solution. Insufficient addition of Triton causes line non-continuity induced by the high surface tension of the liquid. In contrast, higher concentration of Triton often induces residual material between the patterned lines. The PEDOT:PSS wire transistors were tested with Agilent 4156A Precision Semiconductor Parameter Analyzer (Yokogawa-Hewlett-

Packard Ltd, Tokyo, Japan).

Analysis of molecule alignment and electric conductivity: To analyse electric conductivity, a 90 nm-thick PEDOT:PSS film was spin-coated onto SiO_2 (300nm) / Si substrate and annealed at 100°C for 10min. PEDOT:PSS wires were fabricated using the method developed and annealed at the same condition. The Jasco V-670 absorption spectrometer with attached linear polarizer was used to measure the absorption of the patterned PEDOT:PSS wires. The cross-section area of the PEDOT:PSS wires was measured by a profilometer.

ASSOCIATED CONTENT

Data availability. The data that support the findings of this study are available from the corresponding author upon request.

AUTHOR INFORMATION

Corresponding Author

*E-mail. dpc31@cam.ac.uk (D. C.).

Author Contributions

J.L. and X. C. contributed equally to this work, carrying out the experiments and analyzing the data. S. L. designed and carried out the experiments. E.K.W. and P.S helped to optimize the fabrication process. S.L., J.L., X. C. and D.C. prepared the manuscript. D.C. supervised and managed the project.

Notes

The authors declare no competing financial interest.

REFERENCE

(1) Zhang, L.; Liu, H.; Zhao, Y.; Sun, X.; Wen, Y.; Guo, Y.; Gao, X.; Di, C.; Yu, G.; Liu, Y. Inkjet printing high-resolution, large-area graphene patterns by coffee-ring lithography. *Advanced Materials* **2012**, 24, 436−440.

(2) Chen, F. C.; Lu, J. P.; Huang, W. K. Using ink-jet printing and coffee ring effect to fabricate refractive microlens arrays. *IEEE Photonics Technology Letters* **2009**, 21, 648−650.

(3) Farcau, C.; Moreira, H.; Viallet, B.; Grisolia, J.; Ressier, L. Tunable conductive nanoparticle wire arrays fabricated by convective self-assembly on nonpatterned substrates. *ACS nano* **2010**, 4, 7275−7282.

(4) Kim, H. S.; Lee, C. H.; Sudeep, P. K.; Emrick, T.; Crosby, A. J. Nanoparticle stripes, grids, and ribbons produced by flow coating. *Advanced Material*s **2010**, 22, 4600−4604.

(5) Park, J. H.; Lee, D. Y.; Seung, W.; Sun, Q.; Kim, S. W.; Cho, J. H. Metallic grid electrode fabricated via flow coating for high-performance flexible piezoelectric nanogenerators. *The Journal of Physical Chemistry C* **2015**, 119, 7802−7808.

(6) Xu, J.; Xia, J.; Lin, Z. Evaporation-induced self-assembly of nanoparticles from a sphere-on-flat geometry. *Angewandte Chemie International Edition* **2007**, 46, 1860−1863.

(7) Xu, J.; Xia, J.; Hong, S. W.; Lin, Z., Qiu, F.; Yang, Y. Self-assembly of gradient concentric rings via solvent evaporation from a capillary bridge. *Physical review letters* **2006**, 96, 066104.

(8) Lin, Z.; Granick, S. Patterns formed by droplet evaporation from a restricted geometry. *Journal of the American Chemical Society* **2005**, 127, 2816−2817.

(9) Liao, W. S.; Chen, X.; Chen, J.; Cremer, P. S. Templating water stains for nanolithography. *Nano letters* **2007**, 7, 2452−2458.

(10) Byun, M.; Han, W.; Li, B.; Hong, S. W.; Cho, J. W.; Zou, Q.; Lin, Z. Guided Organization of λ-DNA into Microring Arrays from Liquid Capillary Bridges. *Small* **2011**, 7, 1641−1646.

(11) Li, S.; Chun, Y. T.; Zhao, S.; Ahn, H.; Ahn, D.; Sohn, J. I.; Xu, Y.; Shrestha, P.; Pivnenko, M.; Chu, D. High-resolution patterning of solution-processable materials via externally engineered pinning of capillary bridges. *Nature communications* **2018**, 9, 393.

(12) Qing, Q.; Pal, S. K.; Tian, B.; Duan, X.; Timko, B. P.; Cohen-Karni, T.; Murthy, V.N.; Lieber, C. M. Nanowire transistor arrays for mapping neural circuits in acute brain slices. *Proceedings of the National Academy of Sciences* **2010**, 107, 1882−1887.

(13) Qing, Q.; Jiang, Z., Xu, L.; Gao, R.; Mai, L.; Lieber, C. M. Free-standing kinked nanowire transistor probes for targeted intracellular recording in three dimensions. *Nature nanotechnology* **2014**, 9, 142.

(14) van de Burgt, Y.; Lubberman, E.; Fuller, E. J.; Keene, S. T.; Faria, G. C.; Agarwal, S.;

Marinella, M.J.; Talin, A.A.; Salleo, A. A non-volatile organic electrochemical device as a low-voltage artificial synapse for neuromorphic computing. *Nature materials* **2017**, 16, 414.

(15) Isaksson, J.; Kjäll, P.; Nilsson, D.; Robinson, N.; Berggren, M.; Richter-Dahlfors, A. Electronic control of Ca 2+ signalling in neuronal cells using an organic electronic ion pump. *Nature materials* **2007**, 6, 673.

(16) Simon, D. T.; Kurup, S.; Larsson, K. C.; Hori, R.; Tybrandt, K.; Goiny, M.; Jager, E.W.; Berggren, M.; Canlon, B.; Richter-Dahlfors, A. Organic electronics for precise delivery of neurotransmitters to modulate mammalian sensory function. *Nature materials* **2009**, 8, 742.

(17) Campana, A.; Cramer, T.; Simon, D. T.; Berggren, M.; Biscarini, F. Electrocardiographic recording with conformable organic electrochemical transistor fabricated on resorbable bioscaffold. *Advanced Materials* **2014**, 26, 3874−3878.

(18) Gkoupidenis, P.; Schaefer, N.; Garlan, B.; Malliaras, G. G. Neuromorphic functions in PEDOT: PSS organic electrochemical transistors. *Advanced Materials* **2015**, 27, 7176-7180.

(19) Khodagholy, D.; Doublet, T.; Quilichini, P.; Gurfinkel, M.; Leleux, P.; Ghestem, A.; Ismailova, E.; Hervé, T.; Sanaur, S.; Bernard, C.; Malliaras, G.G.   In vivo recordings of brain activity using organic transistors. *Nature communications* **2013**, 4, 1575.

(20) Khodagholy, D.; Rivnay, J.; Sessolo, M.; Gurfinkel, M.; Leleux, P.; Jimison, L. H.; Stavrinidou, E.; Herve, T.; Sanaur, S.; Owens, R.M.;   Malliaras, G. G. High transconductance organic electrochemical transistors. *Nature communications* **2013**, 4, 2133.

(21) Kostianovskii, V.; Sanyoto, B.; Noh, Y. Y. A facile way to pattern PEDOT: PSS film as an

electrode for organic devices. *Organic Electronics* **2017**, 44, 99−105.

(22) Ouyang, S.; Xie, Y.; Zhu, D.; Xu, X.; Wang, D.; Tan, T.; Fong, H. H. Photolithographic patterning of PEDOT: PSS with a silver interlayer and its application in organic light emitting diodes. *Organic Electronics* **2014**, 15, 1822−1827.

(23) Charlot, B.; Sassine, G.; Garraud, A.; Sorli, B.; Giani, A.; Combette, P. Micropatterning PEDOT: PSS layers. *Microsystem technologies* **2013**, 19, 895−903.

(24) Radivo, A.; Sovernigo, E.; Caputo, M.; Dal Zilio, S.; Endale, T.; Pozzato, A.; Goldoni, A.; Tormen, M. Patterning PEDOT: PSS and tailoring its electronic properties by water-vapour-assisted nanoimprint lithography. *RSC Advances* **2014**, 4, 34014−34025.

(25) Tseng, S. F.; Hsiao, W. T.; Huang, K. C.; Chiang, D. Electrode patterning on PEDOT: PSS thin films by pulsed ultraviolet laser for touch panel screens. *Applied Physics A* **2013**, 112, 41-47.

(26) Rutledge, S. A.; Helmy, A. S. Etch-Free Patterning of Poly (3, 4-ethylenedioxythiophene)–Poly (styrenesulfonate) for Optoelectronics. *ACS applied materials & interfaces* **2015**, 7, 3940−3948.

(27) Kim, T. G.; Ha, S. R.; Choi, H.; Uh, K.; Kundapur, U.; Park, S.; Lee, C.W.; Lee, S.H.; Kim, J.;   Kim, J. M. Polymerizable Supramolecular Approach to Highly Conductive PEDOT: PSS Patterns. *ACS applied materials & interfaces* **2017**, 9, 19231−19237.

(28) Thourson, S.B.; Payne, C.K. Modulation of action potentials using PEDOT: PSS conducting polymer microwires. *Scientific reports* **2017**, 7, 1−7.

(29) Pisesweerayos, P.; Dangtip, S.; Supaphol, P.; Srikhirin, T. Electrically Conductive Ultrafine

Fibers of PVA-PEDOT/PSS and PVA-AgNPs by Means of Electrospinning. *Advanced Materials Research* **2014**, 1033,1024−1035.

(30) Yoon, S. S.; Khang, D. Y. Roles of Nonionic Surfactant Additives in PEDOT: PSS Thin Films. *The Journal of Physical Chemistry C* **2016**, 120, 29525−29532.

(31) Natali, M.; Popa, A.; Ebels, U.; Chen, Y.; Li, S.; Welland, M.E. Correlated vortex chiralities in interacting permalloy dot patterns. *J. Appl. Phys.* **2004**, 96, 4334−4341.

(32) Chen, Y.; Lebib, A.; Li, S.; Pépin, A.; Peyrade, D.; Natali, M.; Cambril, E. Nanoimprint and micro-contact printing tri-layer processes. *Eur. Phys. J.* A **2000**, 12, 223.

(33) LeMieux, M. C.; Roberts, M.; Barman, S.; Jin, Y. W.; Kim, J. M.; Bao, Z. Self-sorted, aligned nanotube networks for thin-film transistors. *Science* **2008**, 321, 101−104.

(34) Kolodziejczyk, B.; Ng, C. H.; Strakosas, X.; Malliaras, G. G.; Winther-Jensen, B. Light sensors and opto-logic gates based on organic electrochemical transistors. *Materials Horizons* **2018**, 5, 93−98.

(35) Pan, G.; Chen, F.; Hu, L.; Zhang, K.; Dai, J.; Zhang, F. Effective Controlling of Film Texture and Carrier Transport of a High-Performance Polymeric Semiconductor by Magnetic Alignment. *Advanced Functional Materials* **2015**, 25, 5126−5133.

(36) Mohammadi, E.; Zhao, C.; Meng, Y.; Qu, G.; Zhang, F.;Zhao, X.; Mei, J.; Zuo, J.M.; Shukla, D.; Diao, Y. Dynamic-template-directed multiscale assembly for large-area coating of highly-aligned conjugated polymer thin films. *Nature communications* **2017**, 8, 16070.

(37) Rivnay, J.; Inal, S.; Collins, B.A.; Sessolo, M.; Stavrinidou, E.; Strakosas, X.; Tassone, C.;

Delongchamp, D.M.; Malliaras, G.G. Structure control of mixed ionic and electronic transport in conducting polymers. *Nature communications* **2017**, 7, 11287.

(38) Takano, T.; Masunaga, H.; Fujiwara, A.; Okuzaki, H.; Sasaki, T. PEDOT nanocrystal in highly conductive PEDOT:PSS polymer films. *Macromolecules* **2012**, 45, 3859−3865.

(39) Aasmundtveit, K.E.; Samuelsen, E.J.; Inganäs, O.; Pettersson, L.A.A.; Johansson, T.; Ferrer, S. Structural aspects of electrochemical doping and dedoping of poly(3,4-ethylenedioxythiophene). *Synt. Met.* **2000**, 113, 93−97.